Supplementary Information

Heterogeneous hydroformylation of internal olefins over *dh*-BN supported RhCo alloys: Reaction performance modulated by N vacancies

Bowen Qiu, [a, b] Shujuan Liu, [a] Shimin Liu, [a] Xinjiang Cui [a] Dongcheng He, [a] Kang Zhao, [a] Bin Wang, [a] and Feng Shi*[a]

[a] Bowen Qiu, Shujuan Liu, Dongcheng He, Bin Wang, Prof. Dr. X. Cui, and Prof. Dr. F. Shi, State Key Laboratory for Oxo Synthesis and Selective Oxidation, Lanzhou Institute of Chemical Physics, Chinese Academy of Sciences, No.18, Tianshui Middle Road, Lanzhou, 730000, People's Republic of China

[b] Bowen Qiu, University of Chinese Academy of Sciences, No. 19A, Yuquanlu, Beijing, 100049, People's Republic of China

*Corresponding author: Feng Shi: fshi@licp.cas.cn

1. Experimental

All chemicals are used without further purification. BN are purchased Fujian Schnorrall New Material Co., $Co(NO_3)_3 \cdot 6H_2O$, $Rh(acac)(CO)_2$, $Ce(NO_3)_2 \cdot 6H_2O$, $Cu(NO_3)_2 \cdot 9H_2O$, $Ni(NO_3)_2 \cdot 6H_2O$ and $FeCl_3$ is purchased from Innochem, and Isopropanol (AR) are purchased from Kermel (Tianjin, China).

The substrates, including aliphatic olefins and aromatic olefins, as well as solvents, are purchased from Innochem.

1.1 Preparation of *dh*-BN

Pristine 1 g BN powders dispersed in 5g isopropanol are subjected to Ball-Milling to produce *dh*-BN in a planetary ball mill F-P400 with protection under argon atmosphere. The speed of planetary ball mill F-P400 with a frequency of 480 rpm. The degree of defectiveness in *dh*-BN is controlled by the Ball-Milling time. Different *dh*-BN samples with various Ball-Milling times (0, 20, 40, 120, 240 and 480 min) are prepared and named BN, *dh*-20BN, *dh*-40BN, *dh*-120BN, *dh*-240BN and *dh*-480BN, respectively. Structural pulverization and amorphization of *dh*-BN is commensurate with the Ball-Milling time.

1.2 Typical Procedure for Preparation of RhCo/*dh*-BN Catalyst

In a typical preparation, $Rh(acac)(CO)_2$ (0.070 g, 0.2 mmol) and $Co(NO_3)_2 \cdot 6H_2O$ (0.175 g, 0.6mmol) are added to H_2O (4 mL) at room temperature and stirred until complete dissolution. Then, *dh*-120BN (0.1 g) is added and the mixture is stirred for a further 24 h at room temperature. Afterward, centrifuge the solvent of the suspension and vacuum dry the solid at 100 °C for 8 hours. The obtained solid was then calcined under H_2 at 250 °C for 2 h to afford RhCo/*dh*-BN.To prepare other catalysts, the solution is changed to $Ce(NO_3)_2 \cdot 6H_2O$, $Cu(NO_3)_2 \cdot 3H_2O$, $Ni(NO_3)_2 \cdot 6H_2O$ and Fe $(NO_3)_3 \cdot 9H_2O$ metal precursor, and the rest steps remained the same.

1.3 Typical Procedure for Hydroformylation of 2-Octene

A mixture of RhCo/*dh*-BN catalyst (10 mg), 2-octene (0.224 g, 2.0 mmol), and toluene (2.0 mL) is added into a stainless-steel autoclave (100 mL) with a magnetic stir bar. After the autoclave is sealed and purged with CO three times, the pressure of syngas (CO/H_2 = 1:1) is adjusted to 6.0 MPa. Then the reaction mixture is stirred at 90 °C for 12 h. After the reaction finished, the autoclave is cooled to room

temperature, and the pressure is carefully released. Subsequently, the catalyst is removed from the system by centrifugation and analyzed by gas chromatography (Agilent 7890A GC equipped with an HP-5 capillary column the FID detector). Finally, the yield and regioselectivity are obtained by GC analysis using decane as the internal standard.

For recycling, the catalyst was separated by centrifugation, dried under vacuum at 100 °C for 6 h and used directly for the next run. For Hot Filtration, after 6 h of reaction, cool to room temperature, slowly release the pressure, separate the catalyst from the upper solution, and determine the product in the supernatant by gas chromatography.The remaining solution was transferred into a clean autoclave, pressurized with H_2 and CO, and heated again.

The TOF of product were calculated using the following equations:

$$TOF = \frac{n_{product}}{n_{Rh} \times h}$$

Where $n_{product}$ is the number of moles of generated product, n_{Rh} is the number of moles of metallic Rh in practical loading, and is the reaction time.

1.4 Physical characterization

Gas chromatography analysis is performed on Agilent 7890A GC equipped with an HP-5 capillary column and FID detector. GC-MS analysis is in general recorded on an Agilent 5977A MSD GC-MS.

TEM is carried out by using a Tecnai G2 F30 S-Twin transmission electron microscope operating at 300 kV. Single-particle EDX analysis is performed by using a Tecnai G2 F30 S-Twin Field Emission TEM in STEM mode. For TEM investigations, the catalysts are dispersed in ethanol by ultrasonication and deposited on carbon-coated molybdenum grids.

XRD measurements are conducted by a STADIP automated transmission diffractometer (STOE) equipped with an incident beam curved germanium monochromator selecting Cu Kα1 radiation and a 6 ° position sensitive detector (PSD). The XRD patterns are scanned in the 2θ range of 10-80°. For the data interpretation, the software WinXpow (STOE) and the database of Powder Diffraction File (PDF) of the International Centre of Diffraction Data (ICDD) are used.

XPS is obtained using a VG ES-CALAB 210 instrument equipped with a dual Mg/Al anode X-ray source, a hemispherical capacitor analyzer, and a 5 keV Ar+ iron gun. The electron binding energy is referenced to the C 1s peak at 284.8 eV. The

background pressure in the chamber was less than 10−7 Pa. The peaks are fitted by Gaussian–Lorentzian curves after linear background subtraction. For quantitative analysis, the peak area is divided by the element-specific Scofield factor and the transmission function of the analyzer.

The contents of Rh/Co in the catalysts are measured by inductively coupled plasma-atomic emission spectrometry (ICP-AES), using an Iris Advantage Thermo Jarrel Ash device.

Nitrogen adsorption-desorption isotherms are measured at 77 K using American Quantachrome iQ2 automated gas sorption analyzer. The pore-size distribution is calculated by Barrett, Joyner, and Halenda (BJH) method from desorption isotherm.

IR-diffuse reflectance spectra (IR) of samples are analyzed by a Bruker VERTEX 70 FTIR spectrometer.

The electron paramagnetic resonance (EPR) measurements of LCO solid samples are carried out on a JEOL JES-FA200 spectrometer.

2. N_2 adsorption-desorption analysis

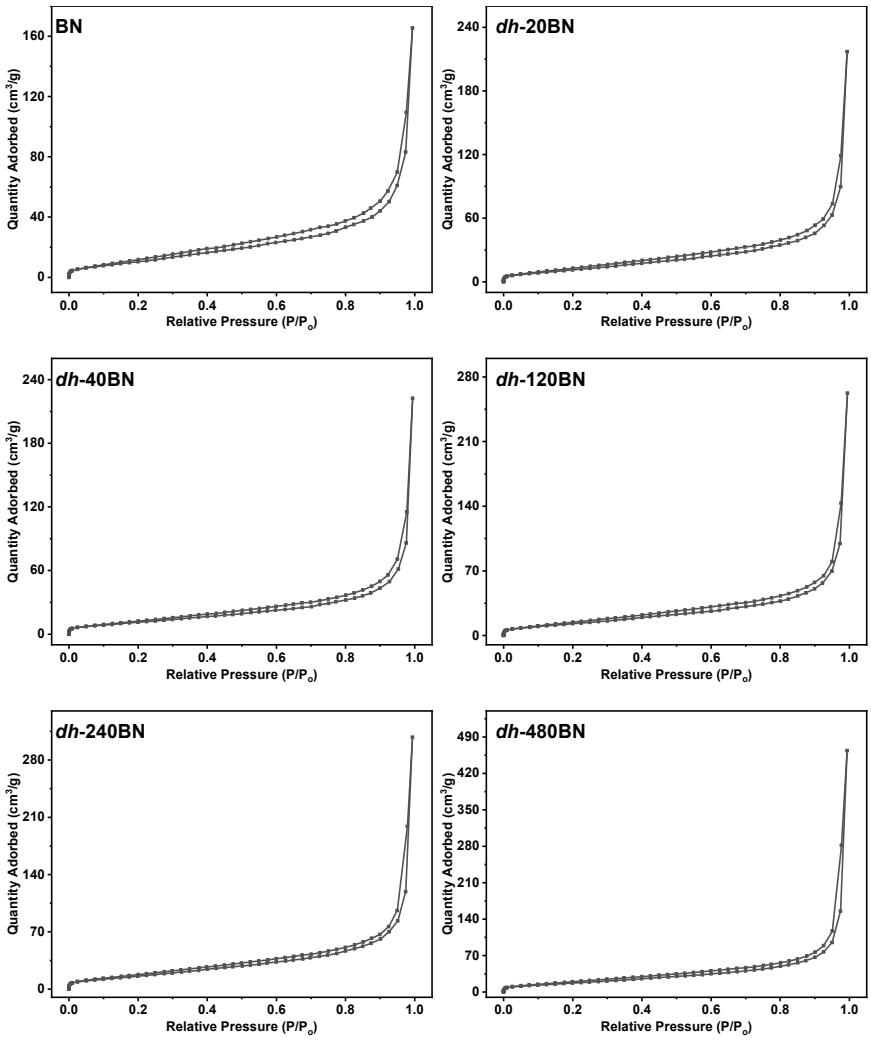

Figure S1 N_2 adsorption-desorption isotherm of the BN and *dh*-BN.

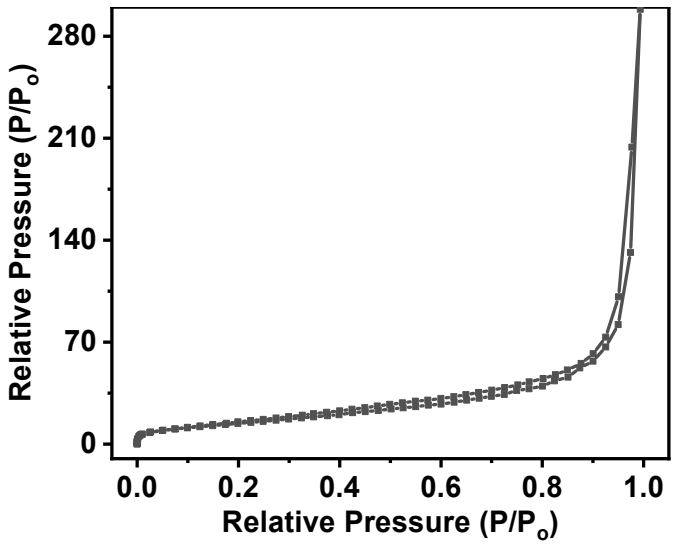

Figure S2 N_2 adsorption-desorption isotherm of the RhCo/*dh*-BN catalyst.

Table S1 The physical properties of catalysts.

Entry	Catalyst	SA (m^2g^{-1})	APW (nm)	PV ($mm^{-3}g^{-1}$)
1	BN	44	0.70	256.4
2	*dh*-20BN	47	0.70	336.3
3	*dh*-40BN	54	0.70	358.8
4	*dh*-120BN	56	1.56	405.8
5	*dh*-240BN	60	1.56	476.1
6	*dh*-480BN	64	1.65	716.9
7	RhCo/*dh*-BN	53	1.66	461.8

Determined by an IQ_2 automated gas sorption analyzer. SA: BET surface area; APS: average pore radius;

PV: pore volume.

3. X-Ray Diffraction analysis

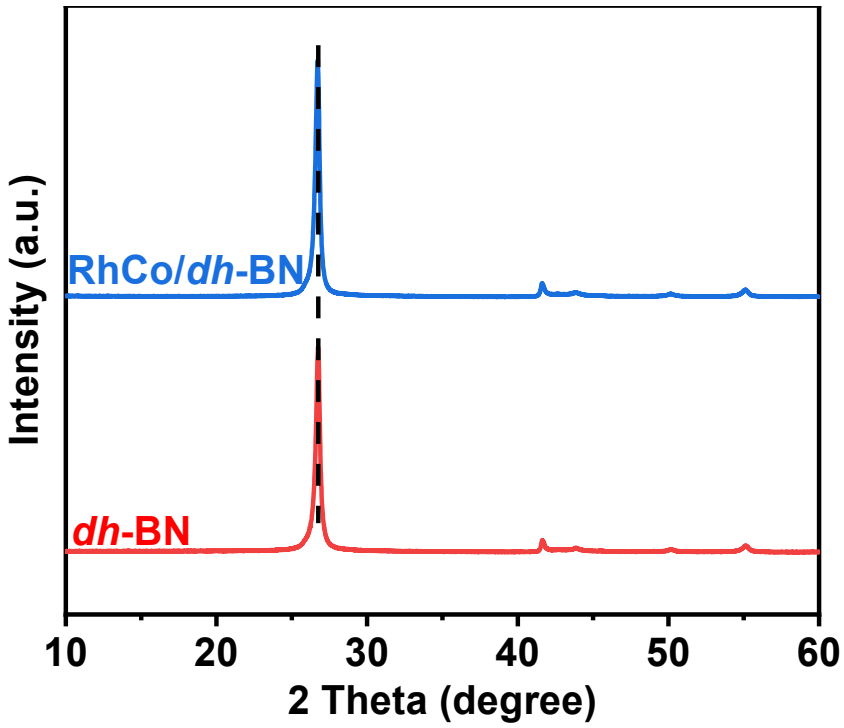

Figure S3 XRD patterns of the samples for *dh*-BN and RhCo/*dh*-BN.

4. X-ray photoelectron spectroscopy analysis

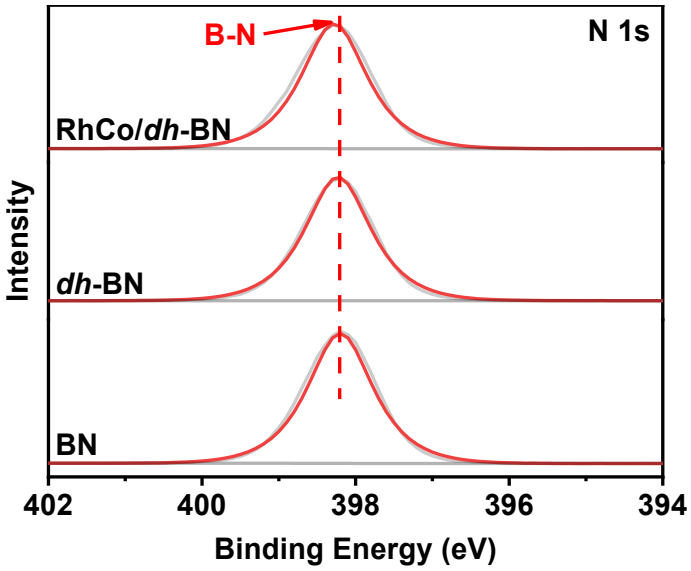

Figure S4 N1s XPS analysis for the catalyst.

5. Transmission electron micrographs

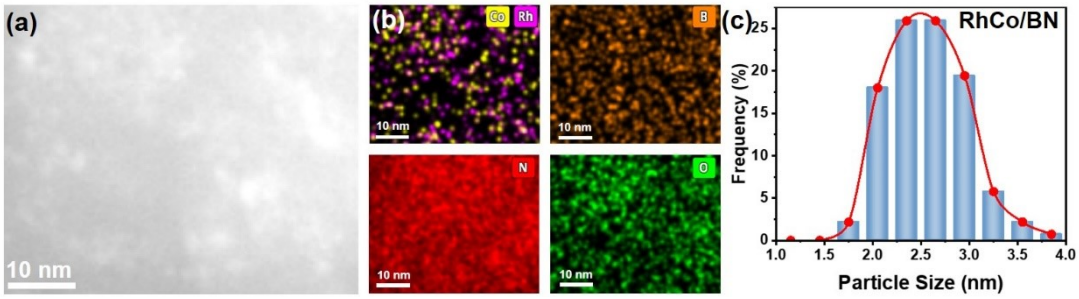

Figure S5 Morphology of RhCo/BN. (a) HAADF- STEM images, (b) EDX elemental mapping, (c) Particle size distribution histogram.

6. Summary of heterogeneous hydroformylation reports in literature

Table S2 Comparison the catalytic performance for hydroformylation of alkenes presented in literatures and this work.

Entry	Catalyst	Substrate	T (°C)	t (h)	P (MPa)	Con./Yield (%)	Sel. (%)	L/B	TOF (h^{-1})	Ref.
1	Rh/RGO	1-hexene	100	1	5	100	72	44/56	508	[1]
2	Rh@UiO-66	1-octene	100	21	5	>99	73	36/64	226	[2]
3	CoRhHT	1-octene	100	6	5	98	96	36/64	6	[3]
4	Rh@CTF	1-octene	80	20	8	68	63	66/34	107	[4]
5	Rh/POL-dppe	1-octene	50	24	1	97	100	29/71	30	[5]
6	Rh–Co–Pi/ZnO	1-decene	100	6	4	97	89	56/44	988	[6]
7	Rh/ZnO@ZIF-8	1-dodecene	90	4.5	4	99	77	48/52	87	[7]
8	CeO_2-R-Rh	styrene	120	8	2	99	97	62/38	72	[8]
9	Rh_1/CeO_2	styrene	120	12	3	99	72	47/53	49	[9]
10	Rh-PAMAM/SiO_2-Fe_3O_4	styrene	50	16	6.9	100	100	3/97	13	[10]
11	Rh/CAM	2-octene	100	5	5	88	-	23/77	559	[11]
12	Rh/Tetraphosphine	2-octene	125	1	1	84	84	98/2	706	[12]
13	RhCo/ BN	2-octene	90	12	6	27	41	68/33	106	This work
14	RhCo/*dh*-BN	2-octene	90	12	6	97	100	0/100	923	This work

Reaction conditions: the ratio of H_2/CO =1:1.

TOF =Moles of converted substrate *(Moles of Rh)$^{-1}$ *(Reaction time h)$^{-1}$.

7. Reaction optimization in hydroformylation of 2-octene.

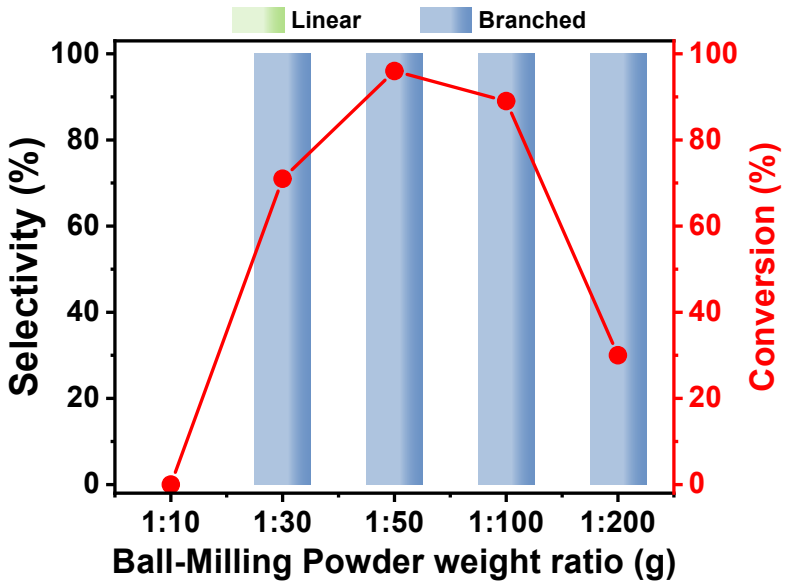

Figure S6 The number of balls optimization in hydroformylation of 2-octene.

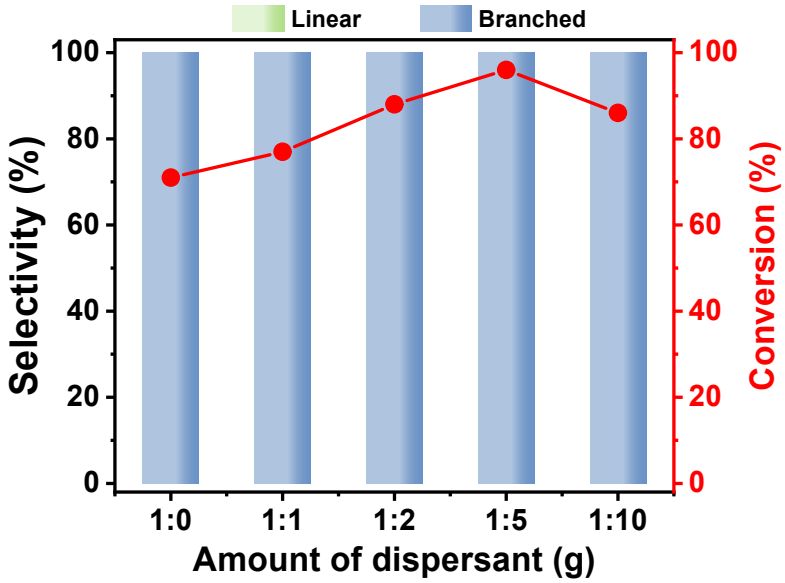

Figure S7 The amount of dispersant optimization in hydroformylation of 2-octene.

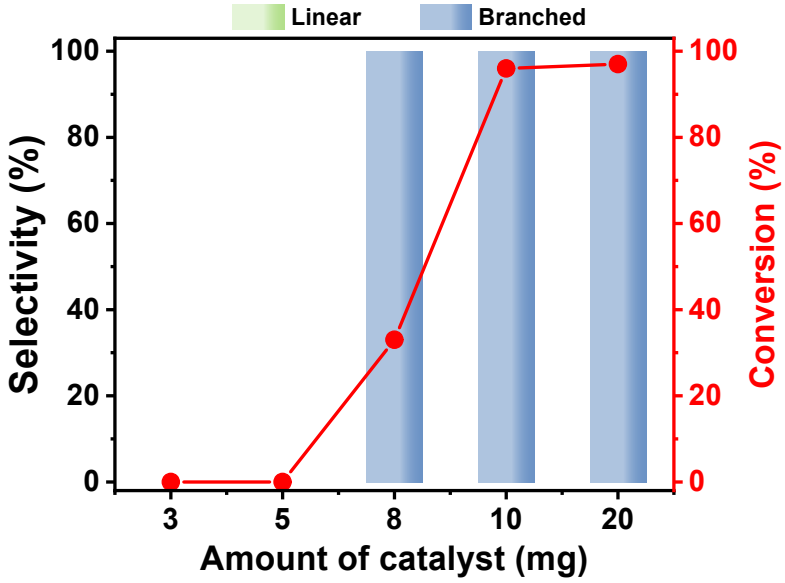

Figure S8 The amount of catalyst optimization in hydroformylation of 2-octene.

6. Characterization of RhCo/*dh*-BN used

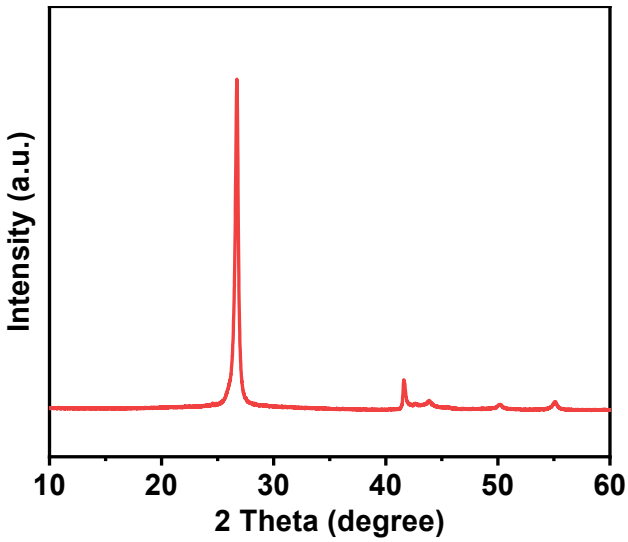

Figure S9 XRD patterns of the samples for RhCo/*dh*-BN used.

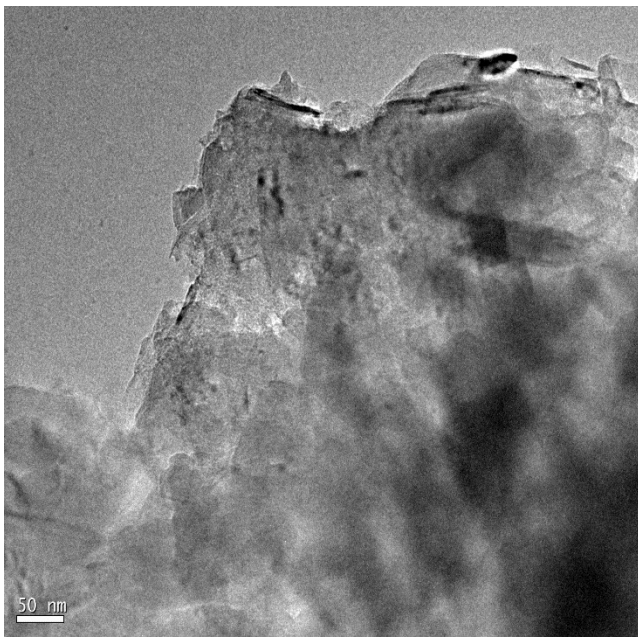

Figure S10 TEM images of the RhCo/*dh*-BN used catalysts.

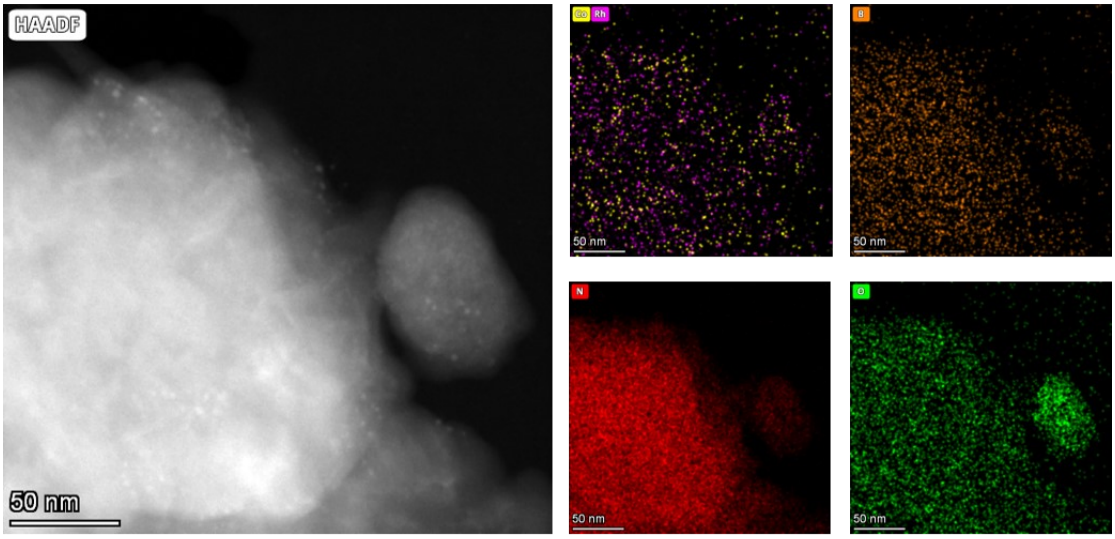

Figure S11 STEM-HAADF images and EDX elemental mapping.

Table S3 Determination of metal content by ICP

Entry	Catalyst	Rh (wt.%)	Co (wt.%)
1	RhCo/*dh*-BN-Fresh	0.18	0.18
2	RhCo/*dh*-BN-Used	0.18	0.18

7. Quantitative GC spectra of the products

Pruduct (1)

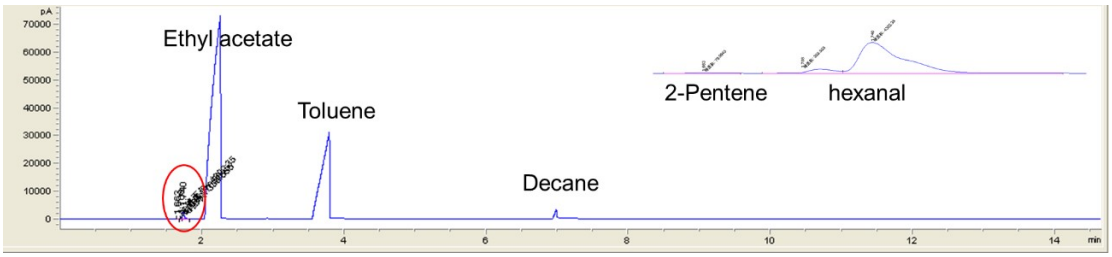

Peak No.	Ret. time	Area	Area%
1	1.663	76.1	1.607
2	1.708	355.6	7.511
3	1.74	4302.3	90.882
Total		4734	100.0000

Pruduct (2)

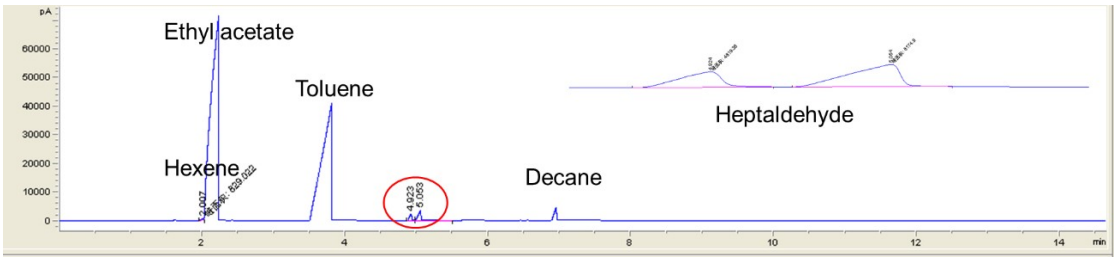

Peak No.	Ret. time	Area	Area%
1	2.007	829	5.997
2	4.924	4819.4	34.864
3	5.054	8174.9	59.139
Total		13823.3	100.0000

Pruduct (3)

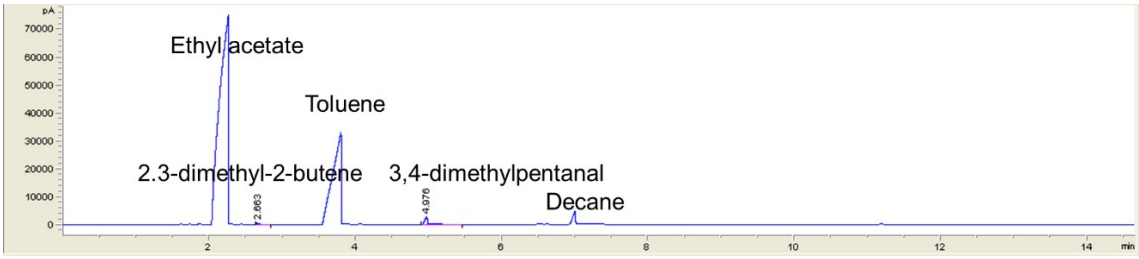

Peak No.	Ret. time	Area	Area%
1	2.663	729.3	8.579
2	4.976	7771.5	91.421
Total		8500.8	100.0000

Pruduct (4)

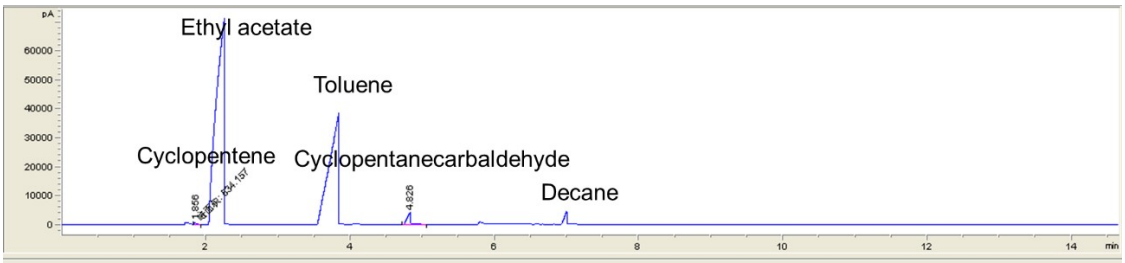

Peak No.	Ret. time	Area	Area%
1	1.856	834.2	6.030
2	4.826	12998.6	93.970
Total		13832.8	100.0000

Pruduct (5)

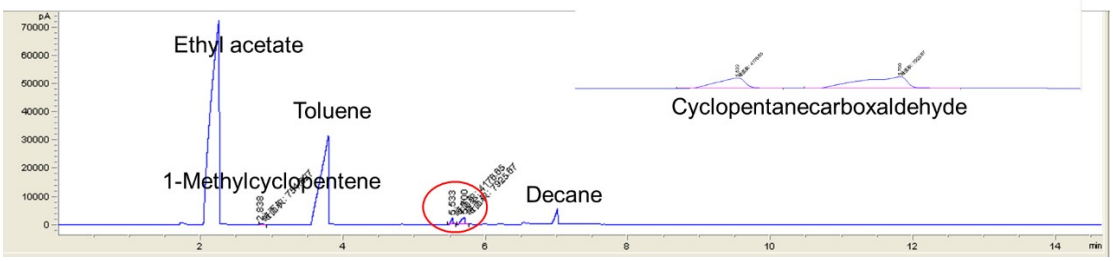

Peak No.	Ret. time	Area	Area%
1	2.838	751.8	5.849
2	5.533	4176.7	32.493
3	5.7	7925.7	61.658
Total		16154.2	100.0000

Pruduct (6)

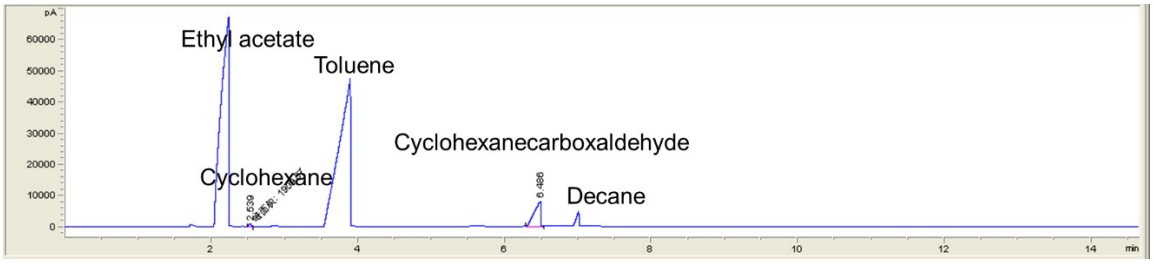

Peak No.	Ret. time	Area	Area%
1	2.639	1909.9	3.844
2	6.486	47770.6	96.156
Total		49680.5	100.0000

Pruduct (7)

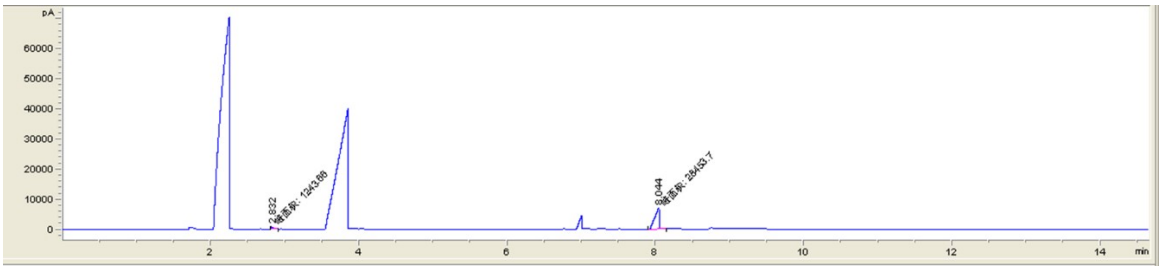

Peak No.	Ret. time	Area	Area%
1	2.832	1243.7	4.188
2	8.044	28453.7	95.812
Total		29697.4	100.0000

Pruduct (8)

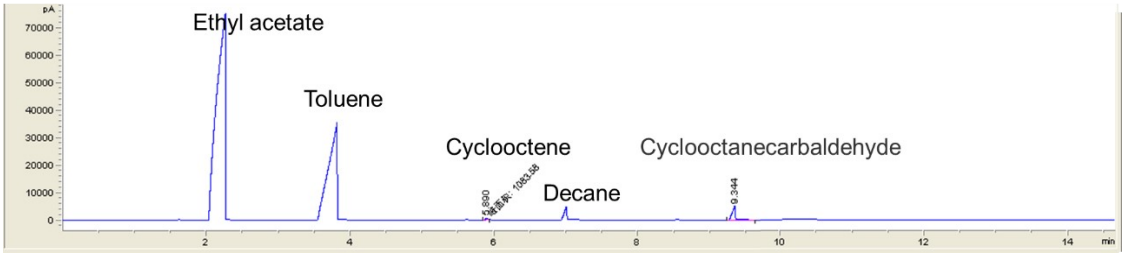

Peak No.	Ret. time	Area	Area%
1	5.89	1083.6	6.467
2	9.344	15670.8	93.533
Total		16754.4	100.0000

Pruduct (9)

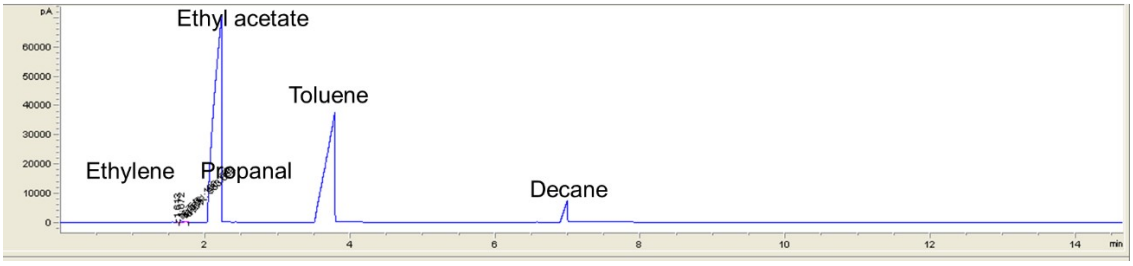

Peak No.	Ret. time	Area	Area%
1	1.613	166.2	14.452
2	1.672	983.7	85.548
Total		1149.9	100.0000

Pruduct (10)

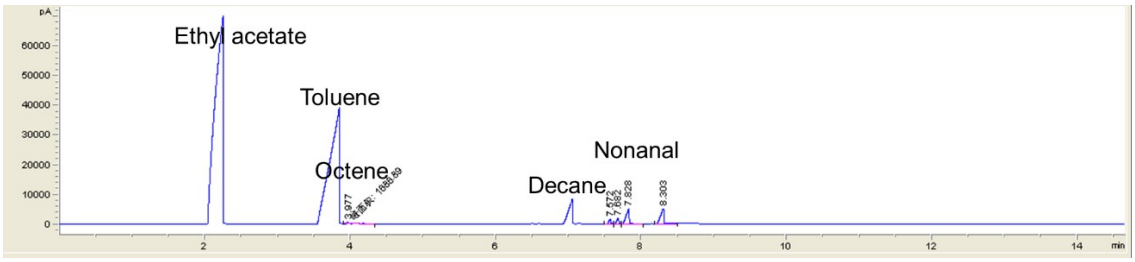

Peak No.	Ret. time	Area	Area%
1	3.977	1686.9	4.305
2	7.572	2885.1	7.363
3	7.682	3779.9	9.847
4	7.828	14233.8	36.326
5	8.303	16597.7	42.359
Total		1149.9	100.0000

Pruduct (11)

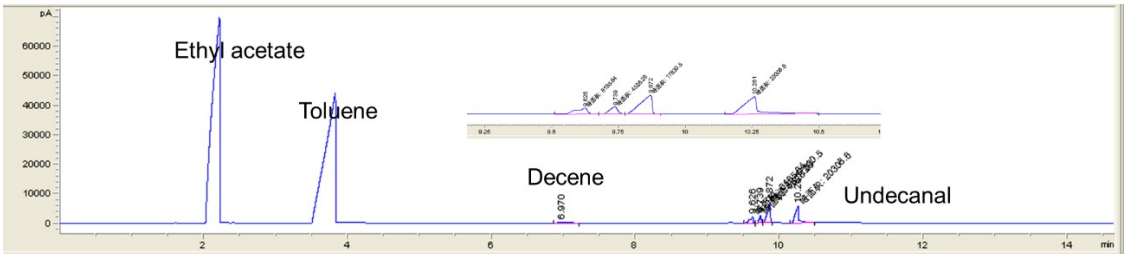

Peak No.	Ret. time	Area	Area%
1	6.97	963.9	1.936
2	9.626	6165.6	12.382
3	9.739	4528.3	9.093
4	9.872	17830.5	35.806
5	10.261	20308.6	40.783
Total		49796.9	100.0000

Pruduct (12)

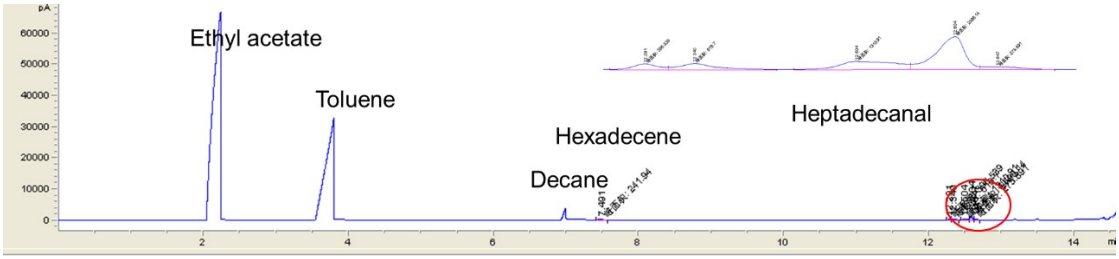

Peak No.	Ret. time	Area	Area%
1	7.491	241.9	4.449
2	12.291	396.5	7.292
3	12.34	616.7	11.340
4	12.504	1310.9	24.106
5	12.604	2596.1	47.740
6	12.647	275.9	5.073
Total		5438	100.0000

Pruduct (13)

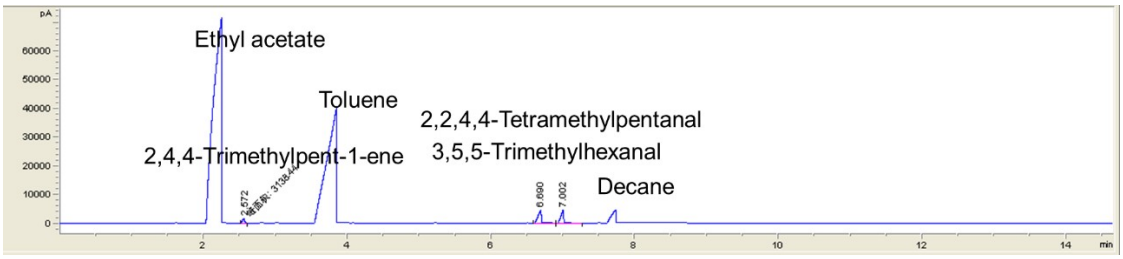

Peak No.	Ret. time	Area	Area%
1	2.572	3138.4	10.904
2	6.69	13756.4	47.795
3	7.002	11887.3	41.301
Total		28782.1	100.0000

Pruduct (14)

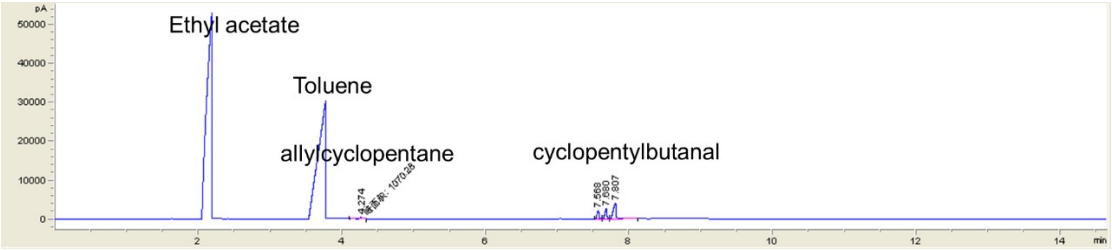

Peak No.	Ret. time	Area	Area%
1	4.274	1070.3	5.068
2	7.568	3767.4	17.841
3	7.68	5098.3	24.143
4	7.807	11180.9	52.948
Total		21116.9	100.0000

8. Quantitative NMR spectra of the products

Pruduct (15)

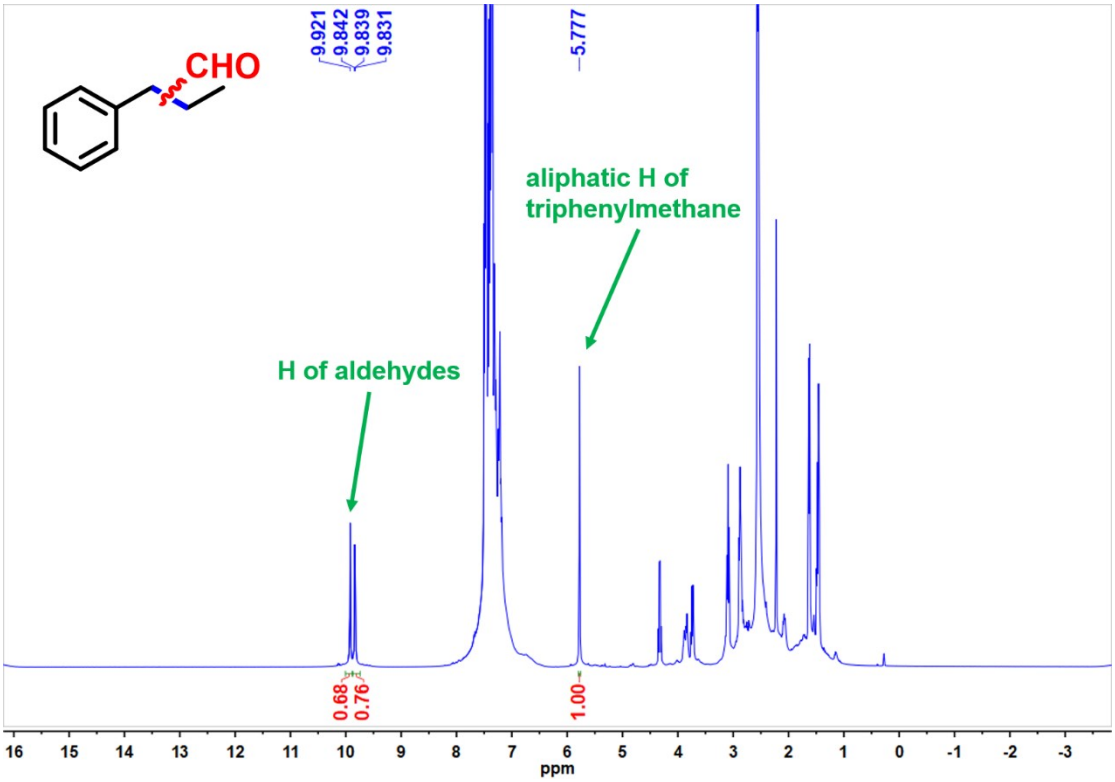

Pruduct (16)

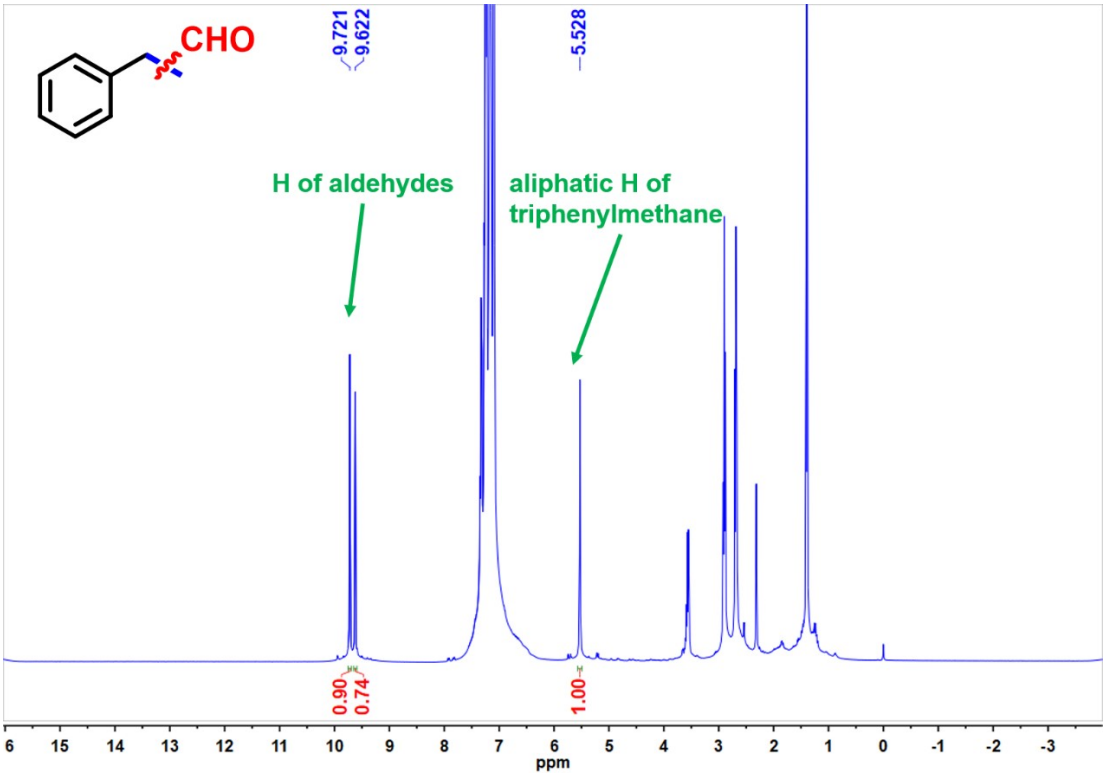

Pruduct (17)

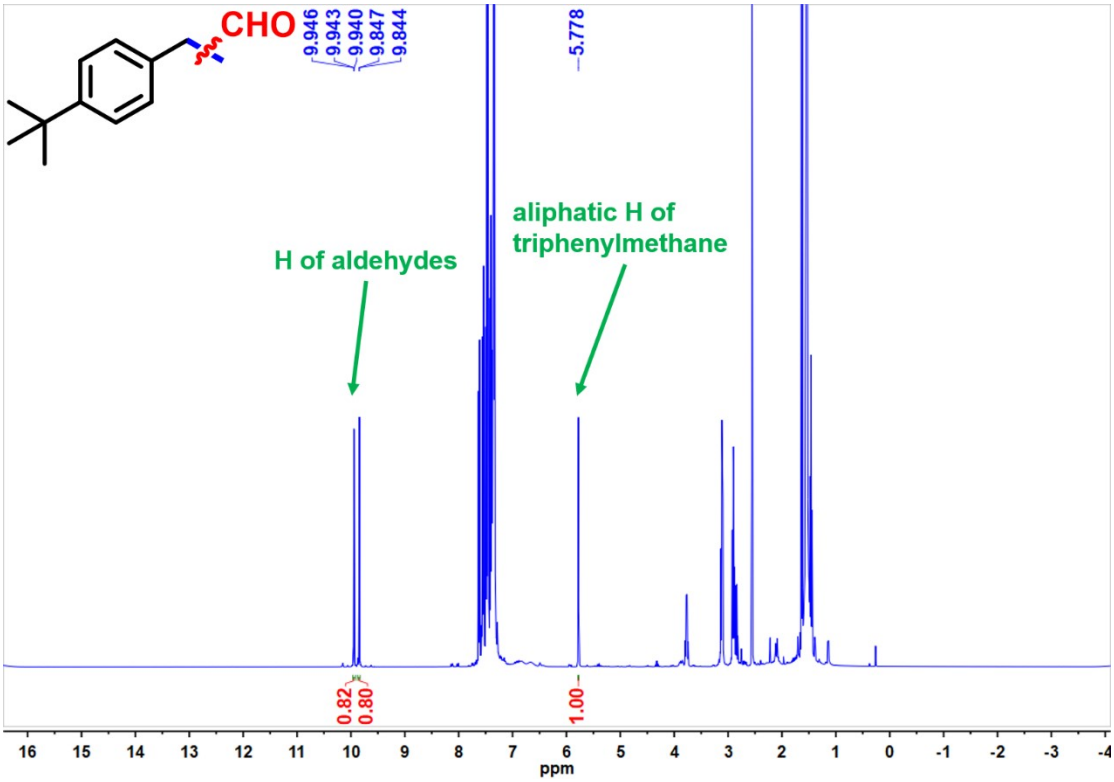

Pruduct (18)

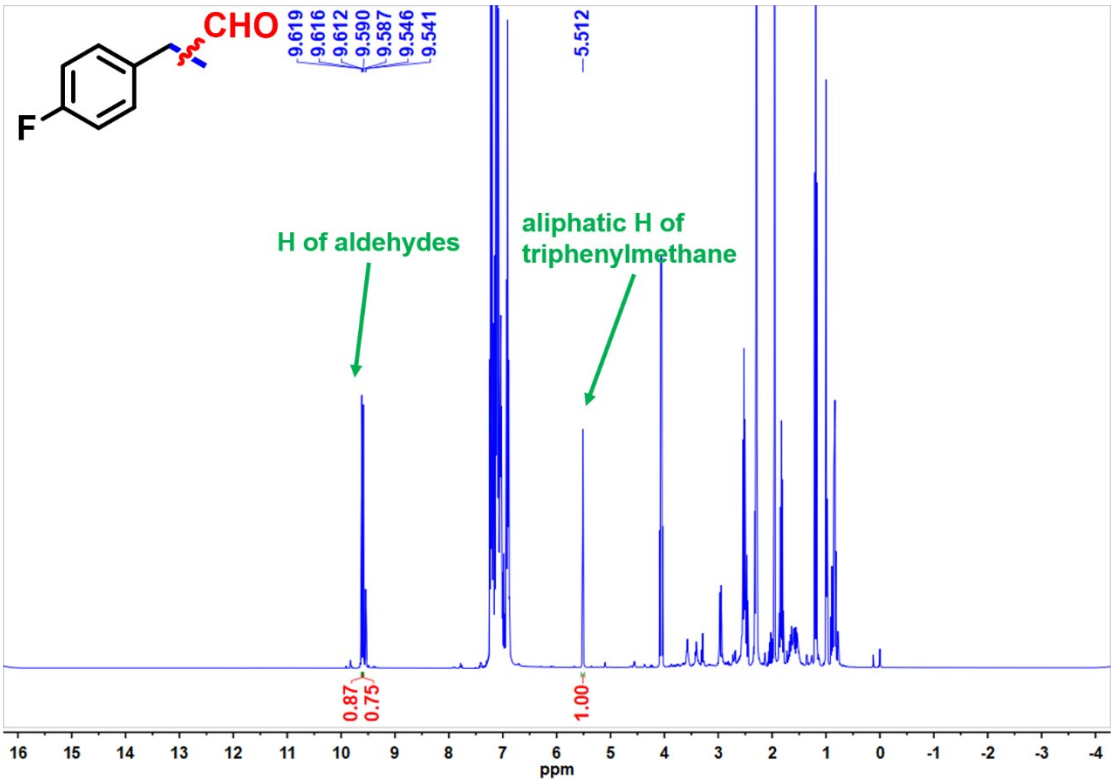
CHO
F
9.619
9.616
9.612
9.590
9.587
9.546
9.541
5.512
H of aldehydes
aliphatic H of
triphenylmethane
0.87
0.75
1.00
16 15 14 13 12 11 10 9 8 7 6 5 4 3 2 1 0 -1 -2 -3 -4
ppm

Pruduct (19)

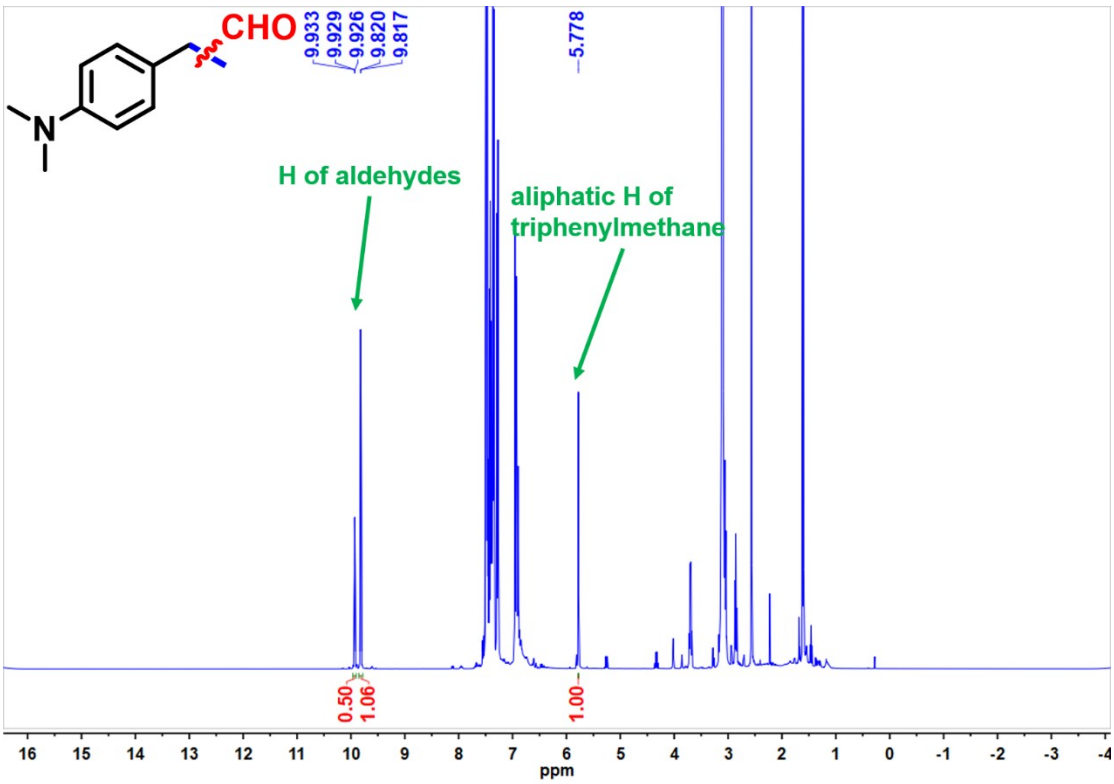
CHO
N
9.933
9.929
9.926
9.820
9.817
5.778
H of aldehydes
aliphatic H of
triphenylmethane
0.50
1.06
1.00
16 15 14 13 12 11 10 9 8 7 6 5 4 3 2 1 0 -1 -2 -3 -4
ppm

Pruduct (20)

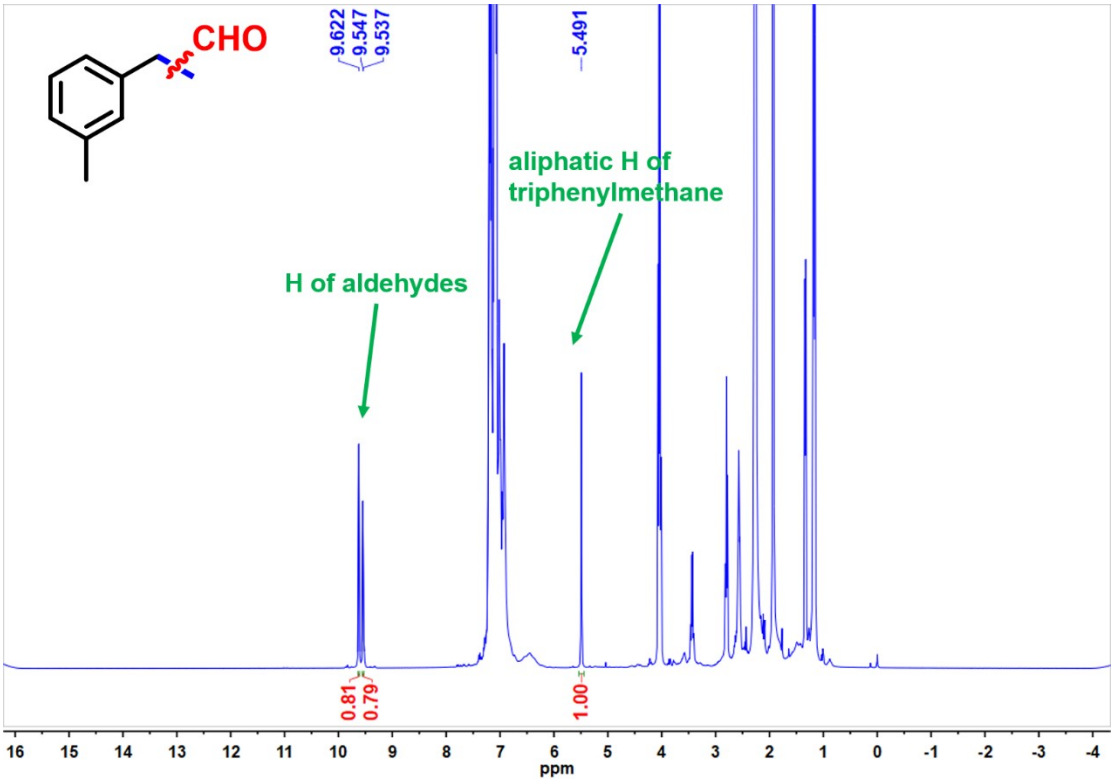

Pruduct (21)

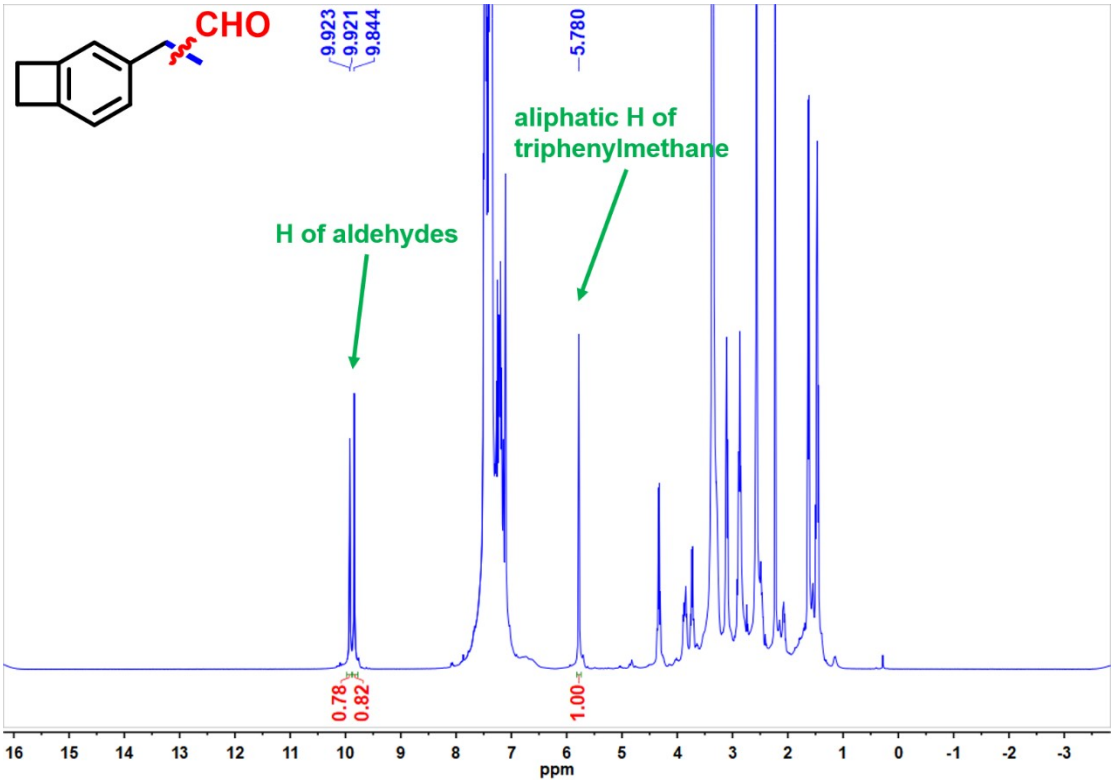

Pruduct (22)

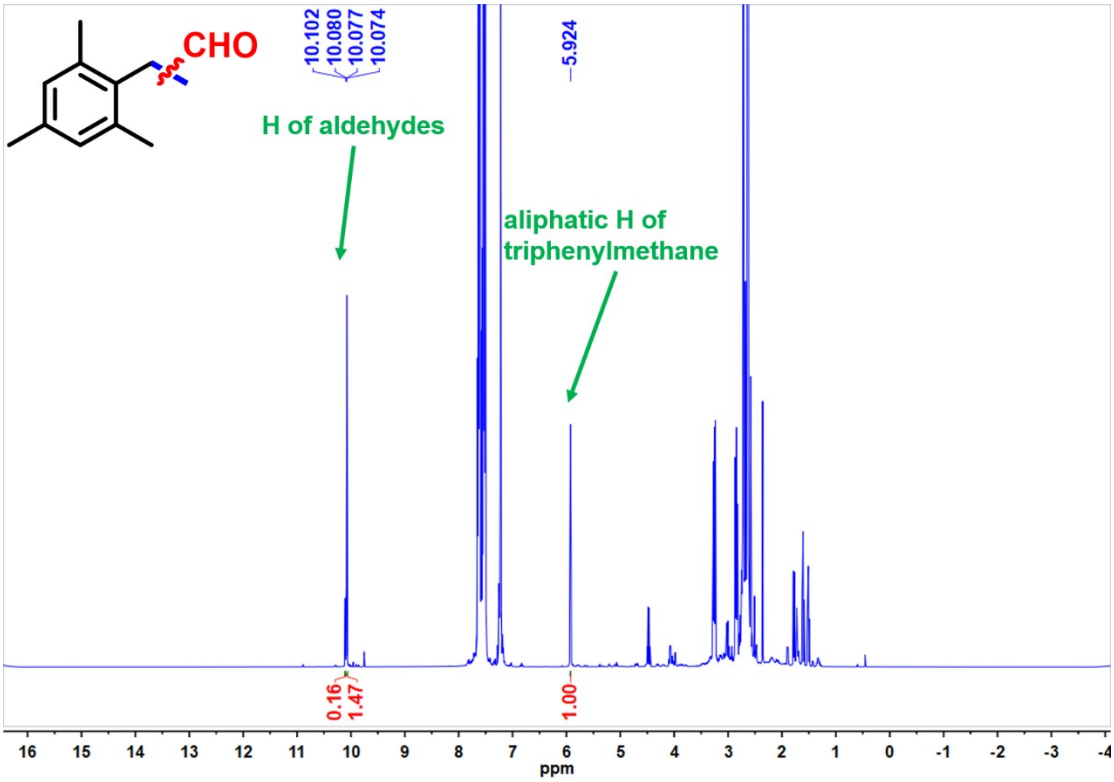

Pruduct (23)

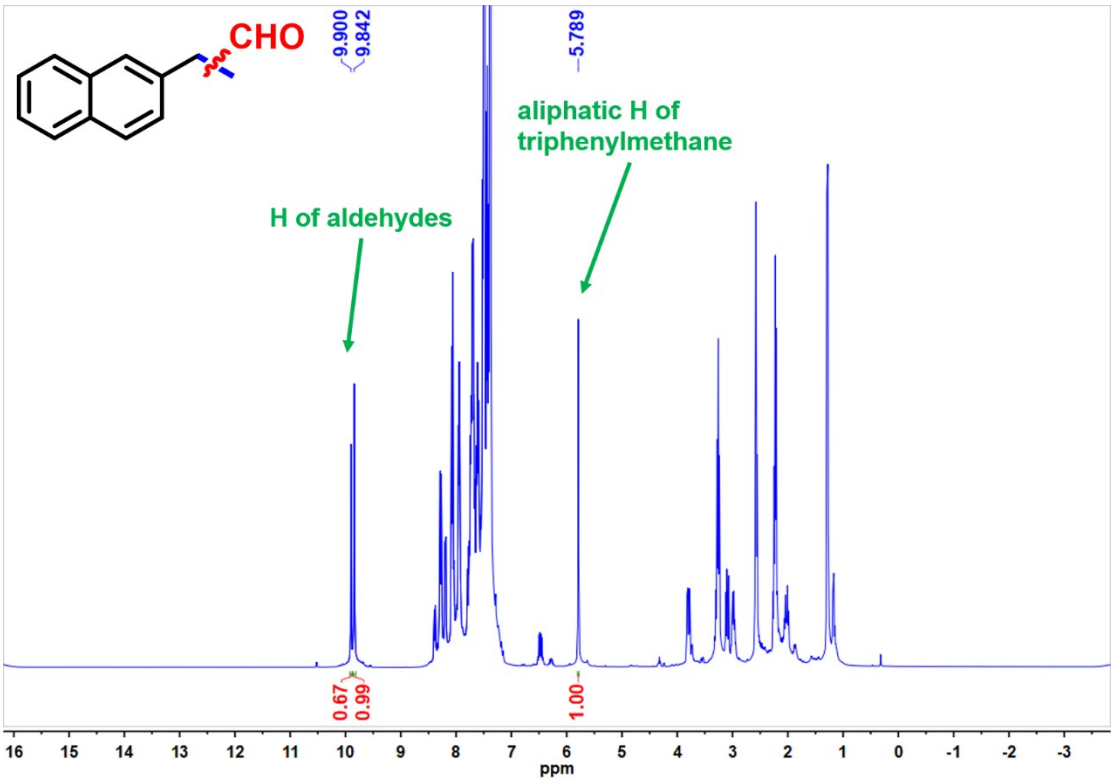

Pruduct (24)

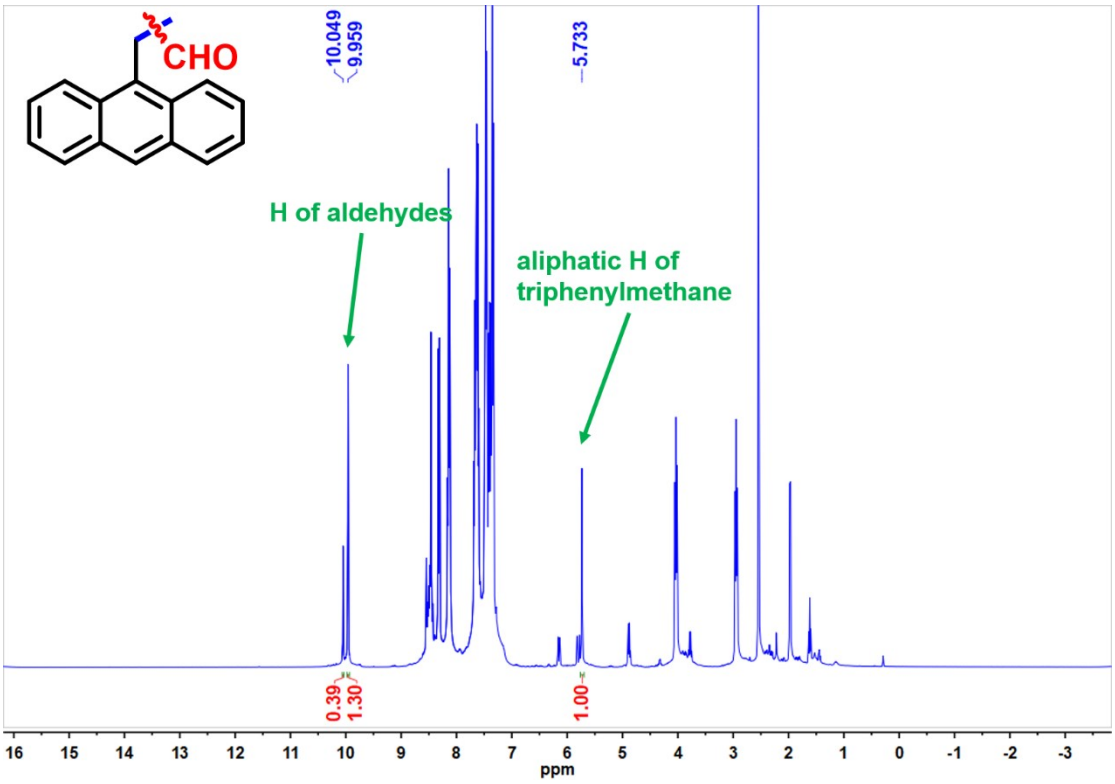
CHO
10.049
9.959
5.733
H of aldehydes
aliphatic H of
triphenylmethane
0.39
1.30
1.00
16 15 14 13 12 11 10 9 8 7 6 5 4 3 2 1 0 -1 -2 -3
ppm

Pruduct (25)

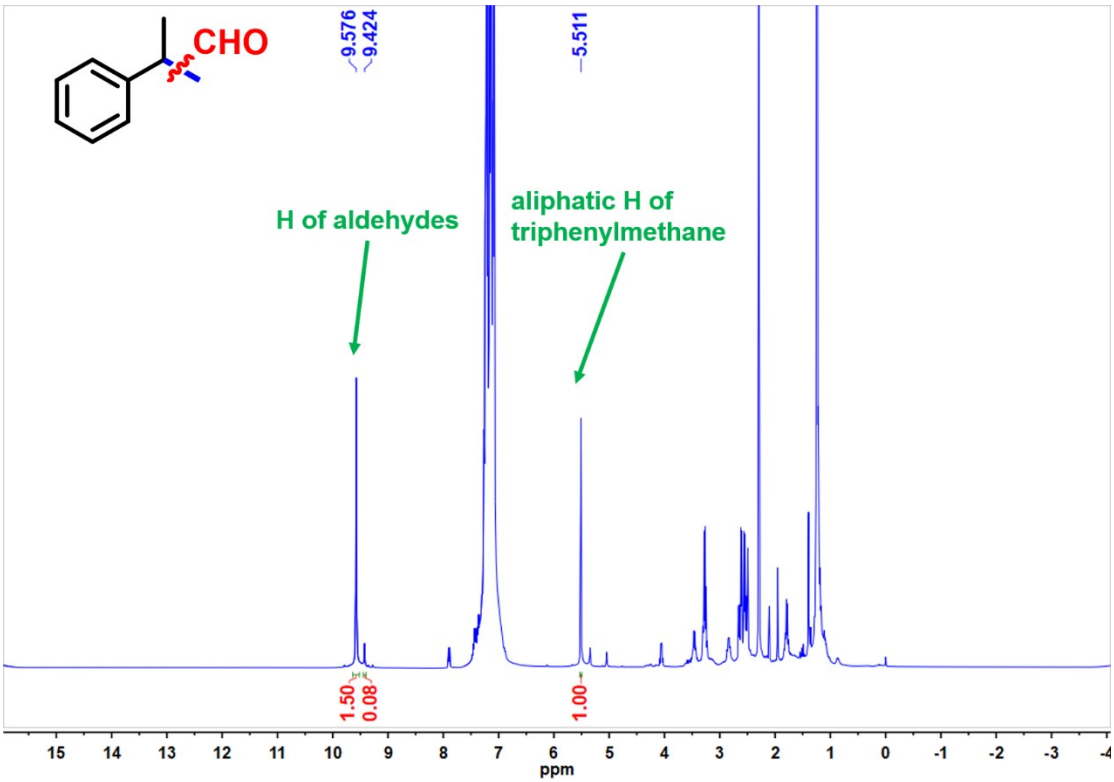

Pruduct (26)

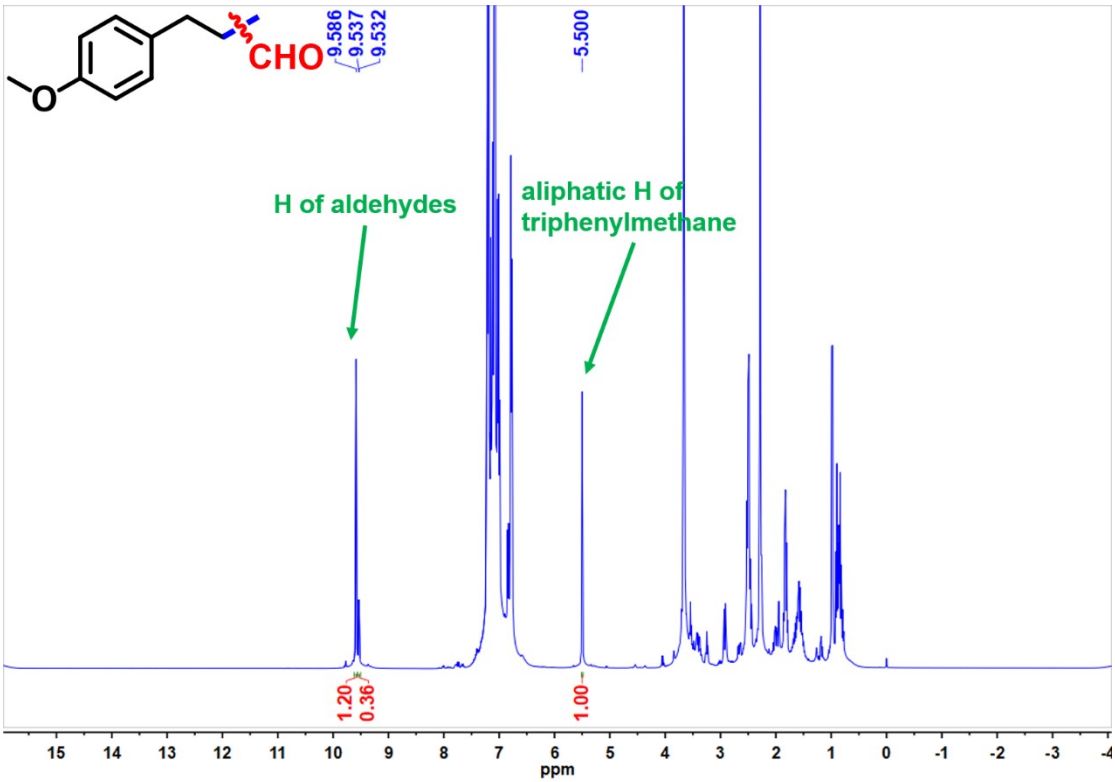

Pruduct (27)

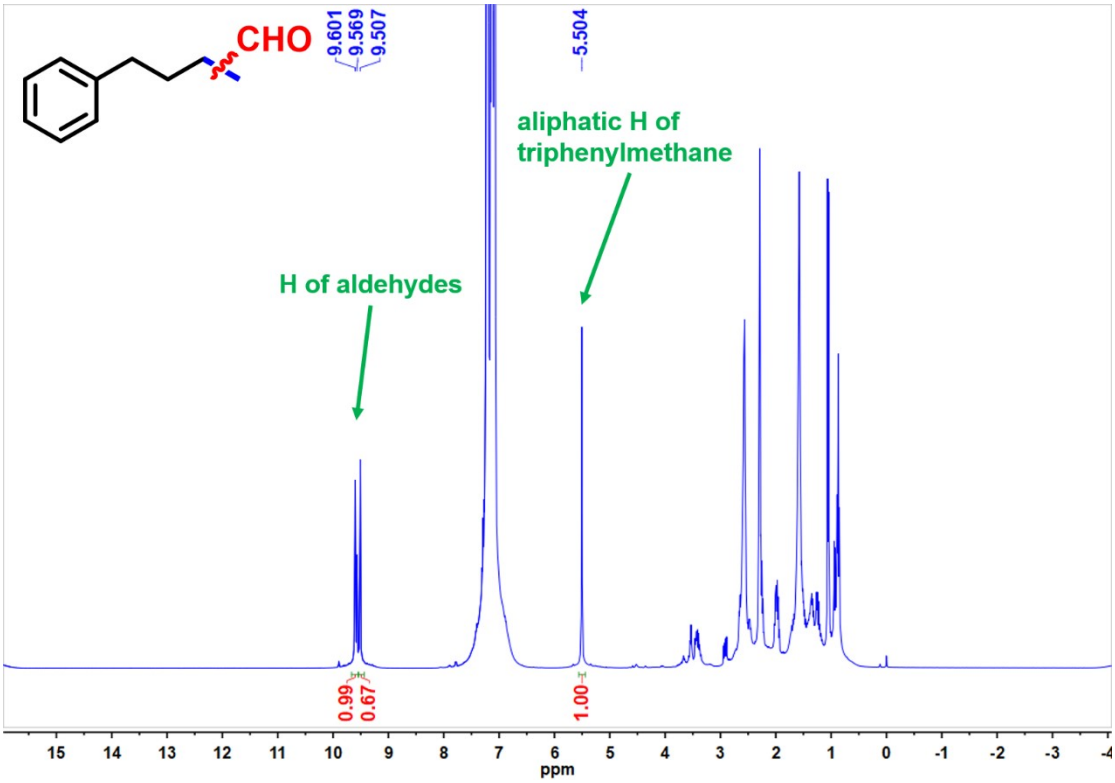

Pruduct (28)

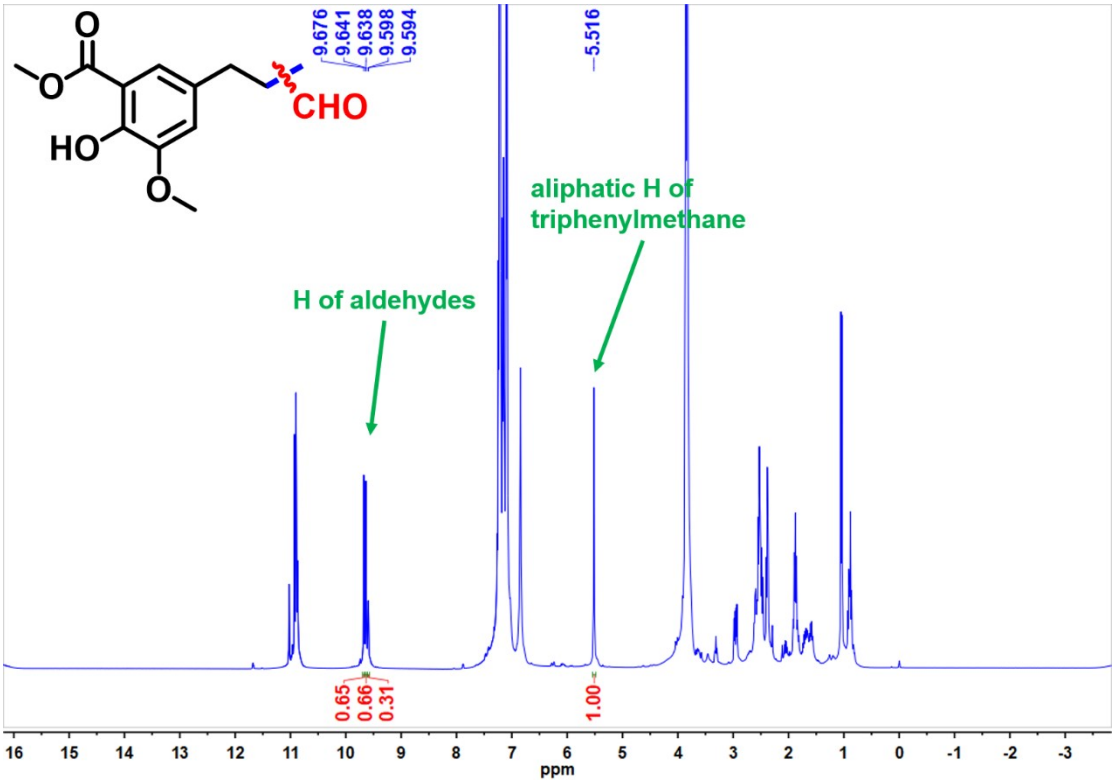

Pruduct (29)

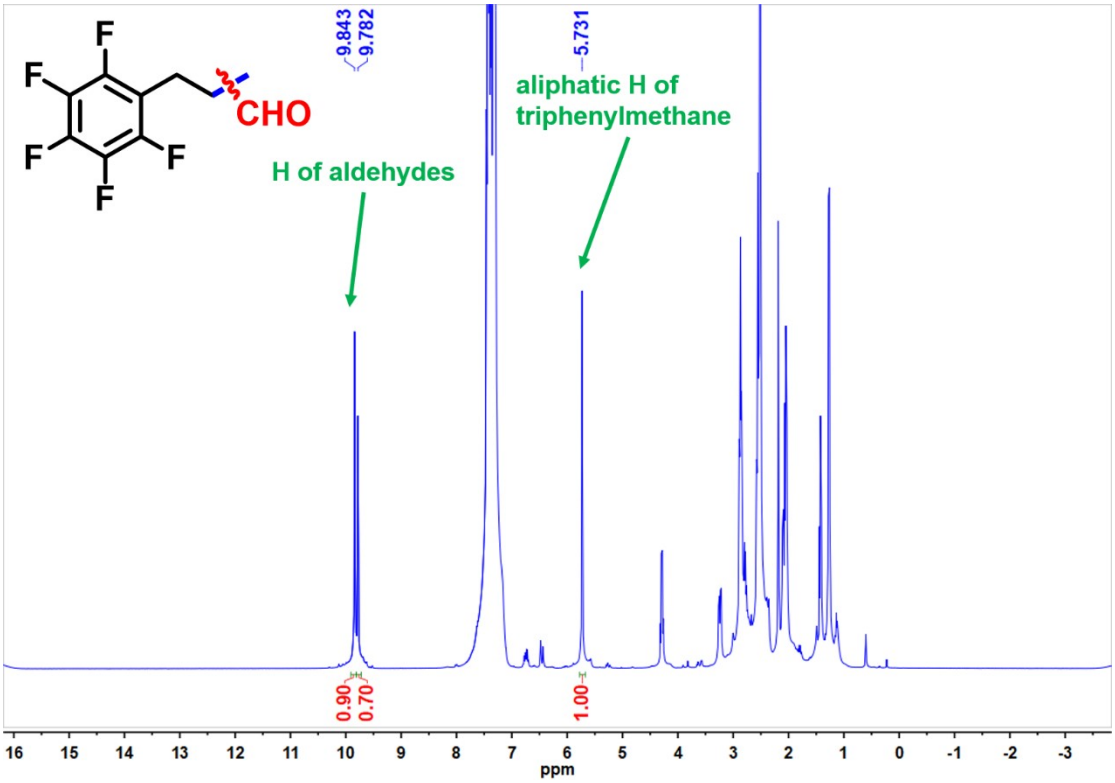
F
F
F
F
F
CHO
9.843
9.782
5.731
aliphatic H of
triphenylmethane
H of aldehydes
0.90
0.70
1.00
16 15 14 13 12 11 10 9 8 7 6 5 4 3 2 1 0 -1 -2 -3
ppm

References

[1] M. Tan, G. Yang, T. Wang, T. Vitidsant, J. Li, Q. Wei, P. Ai, M. Wu, J. Zheng, N. Tsubaki, *Catal. Sci. Technol* **2016**, *6*, 1162-1172.

[2] Y. Sun, J. Harloff, H. Kosslick, A. Schulz, C. Fischer, S. Bartling, M. Frank, A. Springer, *Molecular Catalysis* **2022**, *517*, 112005.

[3] D. Sharma, V. Ganesh, A. Sakthivel, *Appl Catal A-gen.* **2018**, *555*, 155-160.

[4] M. Pilaski, J. Artz, H.-U. Islam, A. M. Beale, R. Palkovits, *Microporous Mesoporous Mater.* **2016**, *227*, 219-227.

[5] Q. Sun, Z. Dai, X. Liu, N. Sheng, F. Deng, X. Meng, F.-S. Xiao, *J. Am. Chem. Soc.* **2015**, *137*, 5204-5209.

[6] B. Wei, X. Liu, K. Hua, Y. Deng, H. Wang, Y. Sun, *ACS Appl. Mater. Interfaces* **2021**, *13*, 15113-15121.

[7] L. Chen, J. Tian, H. Song, Z. Gao, H. Wei, W. Wang, W. Ren, *RSC Advances* **2020**, *10*, 34381-34386.

[8] G. Zeng, Y. Zheng, G. He, C. Zhang, H. Chen, L. Liang, P. Liu, J. Ma, Z. Dong, *Industrial & Engineering Chemistry Research* **2024**, *63*, 2958-2968.

[9] T. Li, F. Chen, R. Lang, H. Wang, Y. Su, B. Qiao, A. Wang, T. Zhang, *Angew. Chem. Int. Ed.* **2020**, *59*, 7430-7434.

[10] R. Abu-Reziq, H. Alper, D. Wang, M. L. Post, *J. Am. Chem. Soc.* **2006**, *128*, 5279-5282.

[11] V. Zakharov, Y. Kardasheva, V. Chernyshev, M. Terenina, K. Kalmykov, D. Ovsyannikov, S. Savilov, S. Filippova, E. Karakhanov, S. Dunaev, L. Aslanov, *Molecular Catalysis* **2023**, *550*, 113598.

[12] C. Cai, S. Yu, G. Liu, X. Zhang, X. Zhang, *Adv. Synth. Catal.* **2011**, *353*, 2665-2670.